

A SPECIAL CLASS OF ORTHONORMAL WAVELETS : THEORY, IMPLEMENTATIONS, AND APPLICATIONS

Lixin Shen, Jo Yew Tham, Seng Luan Lee, and Hwee Huat Tan*

Wavelets Strategic Research Programme
Department of Mathematics
National University of Singapore
10 Kent Ridge Crescent, Singapore 119260
E-mails: {shenlx, thamjy, matleesl, mattanhhh}@wavelets.math.nus.edu.sg

ABSTRACT

This paper introduces a novel class of length- $4N$ orthonormal scalar wavelets, and presents the theory, implementational issues, and their applications to image compression. We first give the necessary and sufficient conditions for the existence of this class. The parameterized representation of filters with different lengths are then given. Next, we derive new and efficient decomposition and reconstruction algorithms specifically tailored to this class of wavelets. We will show that the proposed discrete wavelet transformations are orthogonal and have lower computational complexity than conventional octave-bandwidth transforms using Daubechies' orthogonal filters of equal length. In addition, we also verify that symmetric boundary extensions can be applied. Finally, our image compression results further confirm that improved performance can be achieved with lower computational cost.

1. INTRODUCTION

Orthogonality, smoothness, compact support, and symmetry of wavelet basis are very important properties in filter design. Orthogonality is useful because it means that rate-distortion optimal quantization strategies may be employed in the transform domain and still lead to optimal time-domain quantization (at least when the error is measured in a mean-square sense). The smoothness of wavelets controls the noise in regions with constant background [5]. Also, a higher degree of smoothness corresponds to better frequency localization of the filters [1]. If wavelets are compactly supported, the corresponding lowpass and highpass filters have finite impulse responses, so that the summations in the fast wavelet transform are finite. Symmetry allows the use of symmetric extension to process image borders. As we know, except the Haar basis, all real orthogonal wavelet bases with compact support are asymmetric [1]. On the other hand, smoother wavelets correspond to larger support lengths; consequently, it will increase the computational complexity. The question now is: Can we construct a class of orthonormal wavelets that are smoother, compactly supported, and have low-complexity decomposition and reconstruction implementations?

This paper will show that the above question is not only possible, but also illustrate that better image compression performances

can be achieved with lower computations. In addition, symmetry boundary extensions can be applied for this class of orthonormal wavelets; hence there are no border effects in the decoded images.

2. PARAMETERIZATION OF A SPECIAL CLASS OF LENGTH- $4N$ ORTHONORMAL FILTER BANKS

Let $H_0(z)$ and $H_1(z)$ be the z -transform of the lowpass and high-pass filters associated with an orthonormal scalar wavelet. They are conjugate quadrature (CQF) and power complementary filters [6], i.e. $H_1(z) = -z^{2N+1}H_0(-z)$ and $|H_0(z)|^2 + |H_1(z)|^2 = 1$. The polyphase components of $H_0(z)$ will be denoted by $H_{00}(z)$ and $H_{01}(z)$ such that

$$H_0(z) = H_{00}(z^2) + z^{-1}H_{01}(z^2) = \frac{1}{\sqrt{2}} \sum_{k=0}^{2N-1} h_k z^{-k}.$$

The polyphase components give the even and odd indexed coefficients of $H_0(z)$ separately. Similarly, the polyphase components of $H_1(z)$ will be denoted by $H_{10}(z)$ and $H_{11}(z)$ such that

$$H_1(z) = H_{10}(z^2) + z^{-1}H_{11}(z^2) = \frac{1}{\sqrt{2}} \sum_{k=0}^{2N-1} g_k z^{-k},$$

where $g_k = (-1)^{k+1}h_{2N-1-k}$, $k = 0, 1, \dots, 2N-1$. The polyphase matrix of a scalar wavelet filter can thus be defined as

$$\mathbf{H}_p^N(z) = \begin{bmatrix} H_{00}(z) & H_{10}(z) \\ H_{01}(z) & H_{11}(z) \end{bmatrix}. \quad (1)$$

An important result in [7] is that the polyphase matrix $\mathbf{H}_p^N(z)$ can be factorized as

$$\mathbf{H}_p^N(z) = \mathbf{R}_0 \prod_{j=1}^{N-1} \mathbf{D}(z) \mathbf{R}_j, \quad (2)$$

where

$$\mathbf{D}(z) = \begin{bmatrix} 1 & 0 \\ 0 & z^{-1} \end{bmatrix}, \quad \text{and} \quad \mathbf{R}_j = \begin{bmatrix} \cos \alpha_j & -\sin \alpha_j \\ \sin \alpha_j & \cos \alpha_j \end{bmatrix},$$

for $j = 0, \dots, N-1$. This lattice parameterization gives $\mathbf{H}_p^N(z)$ as a function of angles. Note that $\mathbf{H}_p^N(z)$ is of degree $N-1$. Therefore the filters $H_0(z)$ and $H_1(z)$ are of degree $2N-1$. For

*The author is also with the Department of Electrical Engineering, and a student member of IEEE.

This work was supported by the Wavelets Strategic Research Programme funded by the National Science and Technology Board and the Ministry of Education under Grant RP960 601/A.

the filter to be orthonormal and has at least one vanishing moment, it is necessary that $H_0(1) = 1$ and $H_0(-1) = 0$. Equivalently, these conditions can be expressed in terms of the angles α_j , $j = 0, 1, \dots, N-1$, such that

$$\sum_{j=0}^{N-1} \alpha_j = 2n\pi + \frac{\pi}{4}, \quad n \in \mathbb{Z}. \quad (3)$$

In this paper, we will investigate the construction of a class of orthonormal length- $4N$ scalar wavelet filters $\{h_k\}_{k=0}^{4N-1}$ satisfying

$$h_{2k+1} = (-1)^k h_{2k}, \quad k = 0, 1, \dots, 2N-1. \quad (4)$$

or

$$h_{2k+1} = (-1)^{k+1} h_{2k}, \quad k = 0, 1, \dots, 2N-1. \quad (5)$$

Note that the filter satisfying (5) can be obtained by ‘flipping’ or reversing the order of the filter satisfying (4), and vice versa.

The following theorem provides the necessary and sufficient conditions on the α ’s so that (4) or (5) holds:

Theorem 1. *For any length- $4N$ orthogonal scalar filter $\{h_k\}_{k=0}^{4N-1}$ with the lattice structure (2), it satisfies relation (4) or (5) iff α_j ’s have, respectively, the following properties*

$$\begin{cases} \alpha_{2j} = 2n_j\pi, & j = 1, 2, \dots, N-1, & n_j \in \mathbb{Z}, \\ \alpha_0 = \pi/4, \end{cases} \quad (6)$$

or

$$\begin{cases} \alpha_{2j} = 2n_j\pi, & j = 1, 2, \dots, N-1, & n_j \in \mathbb{Z}, \\ \alpha_0 = 3\pi/4. \end{cases} \quad (7)$$

Proof. Sufficient part: Suppose that α_{2j} satisfy (4) (a similar proof holds for α_{2j} satisfying (5)). Using (2), we obtain

$$H_p^{2N}(z) = R_0 D(z) R_1 \prod_{j=1}^{N-1} D(z^2) R_{2j+1}.$$

Denote $\begin{bmatrix} b_{11}(z^2) & b_{12}(z^2) \\ b_{21}(z^2) & b_{22}(z^2) \end{bmatrix} := \prod_{j=1}^{N-1} D(z^2) R_{2j+1}$. It is clear from (1) that

$$\begin{aligned} H_{00}(z) &= (\cos \alpha_1 - z^{-1} \sin \alpha_1) b_{11}(z^2) + (-\sin \alpha_1 - z^{-1} \cos \alpha_1) b_{12}(z^2), \\ H_{01}(z) &= (\cos \alpha_1 + z^{-1} \sin \alpha_1) b_{11}(z^2) + (-\sin \alpha_1 + z^{-1} \cos \alpha_1) b_{12}(z^2). \end{aligned}$$

Thus, we have $H_{00}(z) = H_{01}(-z)$. This implies that the filter $\{h_k\}_{k=0}^{4N-1}$ satisfies the relation (4).

Necessary part: If an orthogonal scalar filter $\{h_k\}_{k=0}^{4N-1}$ satisfies the relation (4), then the polyphase matrix $H_p^{2N}(z)$ has the form

$$\begin{bmatrix} H_{00}(z) & H_{10}(z) \\ H_{00}(-z) & H_{10}(-z) \end{bmatrix}.$$

In [2], G. Evangelista proved that such a matrix can be factorized as

$$H_p^{2N}(z) = R_0 D(z) R_1 \prod_{j=1}^{N-1} D(z^2) R_{2j+1},$$

where $\alpha_0 = \pi/4$. Using the fact $D(z^2) = D(z)ID(z)$, we have

$$H_p^{2N}(z) = R_0 D(z) R_1 \prod_{j=1}^{N-1} D(z) I D(z) R_{2j+1}.$$

By comparing it with (2), we obtain $R_{2j} = I$. Thus we have $\alpha_{2j} = 2n_j\pi$, $n_j \in \mathbb{Z}$. \square

2.1. Some Examples

From Theorem 1 and equation (3), one can obtain the parameterized length-8 (when $N = 2$) filter as

$$\begin{aligned} h_0 &= -\frac{\sqrt{2}}{4} \sin 2\alpha, h_1 = -h_0, h_2 = \frac{\sqrt{2}}{2} \sin^2 \alpha, h_3 = h_2, \\ h_4 &= \frac{\sqrt{2}}{4} \sin 2\alpha, h_5 = -h_4, h_6 = \frac{\sqrt{2}}{2} \cos^2 \alpha, h_7 = h_6. \end{aligned}$$

Clearly, this filter satisfies relation (5). If the parameter α is not a multiple of π , we can verify that $\inf_{Re(z) \geq 0} |H_0(z)| > 0$. Therefore, the associated wavelet will constitute an orthonormal basis of $L^2(\mathbb{R})$. When $\alpha = \frac{\pi}{2} - \frac{1}{2} \arcsin(\frac{1}{4})$, the filter denoted by S8(1) has two vanishing moments, and the corresponding wavelet has a Hölder exponent of 1.0094. When $\alpha = 1.42616$, the filter denoted by S8(2) has only one vanishing moment, but has optimal transition band with respect to the ideal ‘brickwall’ filter.

For $N = 3$, the parameterized length-12 filter is given by

$$\begin{aligned} h_0 &= \frac{\sqrt{2}}{2} \cos \alpha \cos \beta \cos(\alpha + \beta), \\ h_2 &= -\frac{\sqrt{2}}{2} \sin \alpha \cos \beta \cos(\alpha + \beta), \\ h_4 &= \frac{\sqrt{2}}{2} \sin^2 \beta, h_6 = -\frac{\sqrt{2}}{2} \cos \beta \sin \beta, \\ h_8 &= \frac{\sqrt{2}}{2} \sin \alpha \cos \beta \sin(\alpha + \beta), \\ h_{10} &= \frac{\sqrt{2}}{2} \cos \alpha \cos \beta \sin(\alpha + \beta), \end{aligned}$$

and $h_{2k+1} = (-1)^k h_{2k}$, $k = 0, \dots, 5$. When $\alpha = 1.5229$ and $\beta = 1.6962$, the filter denoted by S12(1) has three vanishing moments, and has a Hölder exponent of 1.0032 (if $\alpha = 4.3752$ and $\beta = 4.8577$, the filter has three vanishing moments, and a Hölder exponent of 1.2814). When $\alpha = 1.5223$ and $\beta = 1.7129$, the filter denoted by S12(2) has one vanishing moment and optimal transition band.

3. NEW MULTIREOLUTION DECOMPOSITION AND RECONSTRUCTION ALGORITHMS AND THEIR PROPERTIES

Given any length- $4N$ CQF $\{h_k\}_{k=-2N+2}^{2N+1}$ that satisfies (4) or (5), we generate a lowpass filter $\{\underline{h}_k\}_{k=-2N+2}^{2N+1}$, and two highpass filters $\{g_k\}_{k=-2N+2}^{2N+1}$ and $\{\underline{g}_k\}_{k=-2N+2}^{2N+1}$, such that

$$\underline{h}_k = h_{3-k}, \quad g_k = (-1)^{k+1} h_{3-k}, \quad \underline{g}_k = g_{3-k}. \quad (8)$$

Obviously, the two scaling functions corresponding to $\{h_k\}_{k=-2N+2}^{2N+1}$ and $\{\underline{h}_k\}_{k=-2N+2}^{2N+1}$ form a symmetric pair at point $\frac{3}{2}$. By equations (4) and (8), it is easy to check the following relations hold:

Proposition 1.

$$\begin{aligned} \sum_k h_k \underline{h}_{k+4\ell} &= 0, & \sum_k h_k \underline{g}_{k+4\ell} &= 0, \\ \sum_k g_k \underline{h}_{k+4\ell} &= 0, & \sum_k g_k \underline{g}_{k+4\ell} &= 0. \end{aligned}$$

For this special class of filter banks, we will present new multiresolution decomposition and reconstruction algorithms which are different from the traditional framework [3].

3.1. The Proposed Decomposition Algorithm

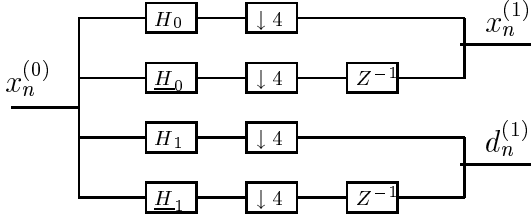


Figure 1: Proposed multiresolution decomposition algorithm.

Let $\{x_n^{(0)}\}$ be the input data. As shown in Figure 1, the decimated outputs after one level of decomposition are the reference signal $\{x_n^{(1)}\}$ and the detail signal $\{d_n^{(1)}\}$, where

$$\begin{aligned} x_{2n}^{(1)} &= \sum_k h_{k-4n} x_k^{(0)}, & x_{2n+1}^{(1)} &= \sum_k \underline{h}_{k-4n} x_k^{(0)}, \\ d_{2n}^{(1)} &= \sum_k g_{k-4n} x_k^{(0)}, & d_{2n+1}^{(1)} &= \sum_k \underline{g}_{k-4n} x_k^{(0)}. \end{aligned}$$

By Proposition 1, such a decomposition scheme generates an orthogonal transformation mapping $\{x_n^{(0)}\} \rightarrow \{x_n^{(1)}, d_n^{(1)}\}$. The representation matrix of the orthogonal transformation \mathbf{P} is orthogonal, i.e. $\mathbf{P}^{-1} = \mathbf{P}^T$. This process is repeated recursively on the reference signal. After L levels, we obtain the reference signal $\{x_n^{(L)}\}$ with a resolution reduced by factor of 2^L with respect to $\{x_n^{(0)}\}$, and the detail signals $\{x_n^{(L)}\}, \dots, \{x_n^{(1)}\}$.

3.2. The Proposed Reconstruction Algorithm

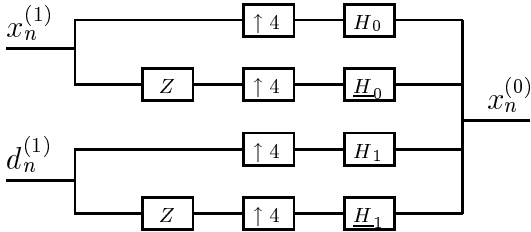


Figure 2: Proposed multiresolution reconstruction algorithm.

Due to the orthogonality of the decomposition transformation, the representation matrix of the reconstruction transformation is just \mathbf{P}^T . Given the level- ℓ reference signal $\{x_n^{(\ell)}\}$ and detail signal $\{d_n^{(\ell)}\}$,

we can reconstruct the reference signal $\{x_n^{(\ell-1)}\}$ at level $\ell-1$ using the following formulae (see Figure 2):

$$\begin{aligned} x_n^{(\ell-1)} &= \sum_k (h_{n-4k} x_{2k}^{(\ell)} + \underline{h}_{n-4k} x_{2k+1}^{(\ell)}) \\ &\quad + \sum_k (g_{n-4k} d_{2k}^{(\ell)} + \underline{g}_{n-4k} d_{2k+1}^{(\ell)}). \end{aligned}$$

Similarly, this process is applied recursively on the reference and detail signals until we recover the original signal $\{x_n^{(0)}\}$.

3.3. Computational Complexity

One important consideration in application is the computational complexity of applying a given filter, which directly relates to its implementational efficiency. For most practical applications, the dominating factor for computational complexity is usually governed by the number of multiplications involved, hence justifying it as a measure of the computational cost of using a wavelet filter.

In general, for a length- $2N$ orthogonal filter (with no symmetry), each output sample will require $2N$ multiplications during decomposition or reconstruction using Mallat's algorithms [3]. By exploiting the specific properties in (4) or (5) and employing the proposed multiresolution algorithms, we can easily show that each output sample now will only require $2N$ multiplications when using a length- $4N$ filter belonging to this special class. As mentioned earlier, longer filters have higher regularity. Hence, this special class of orthonormal wavelets can possess greater smoothness without a penalty on computation complexity.

3.4. Symmetric Boundary Extension

Let $\{h_k\}_{k=2N-2}^{2N+1}$ be a length- $4N$ CQF satisfying (4) or (5), and the filters $\{g_k\}_{k=2N-2}^{2N+1}$, $\{\underline{h}_k\}_{k=2N-2}^{2N+1}$, and $\{\underline{g}_k\}_{k=2N-2}^{2N+1}$ satisfy (8). Although this special class of orthonormal wavelets are not symmetrical, we show that symmetric boundary extension can be applied when using the proposed multiresolution algorithms.

Suppose that $\{x_k^{(0)}\}_{k=0}^{2K-1}$ is an input sequence with an even number of samples. We can perform a half-point symmetric extension as follows:

$$\dots, x_{-2}, x_{-1}, x_0, x_1, \dots, x_{2K-2}, x_{2K-1}, x_{2K}, x_{2K+1}, \dots \quad (9)$$

where

$$x_{-k-1} = x_k \quad \text{and} \quad x_{2K+k} = x_{2K-1-k}. \quad (10)$$

To show that symmetric boundary extension is applicable, we only need to prove that the output signals are also symmetrical; i.e. proving $x_{2n}^{(1)} = x_{-2n-1}^{(1)}$, as follows:

$$\begin{aligned} x_{-2n-1}^{(1)} &= \sum_k \underline{h}_k x_{k+4(-n-1)}^{(0)} = \sum_k h_{3-k} x_{k+4(-n-1)}^{(0)} \\ &= \sum_k h_k x_{3-k+4(-n-1)}^{(0)} = \sum_k h_k x_{-4+k-4(-n-1)}^{(0)} \\ &= x_{2n}^{(1)}. \end{aligned}$$

Similarly, we can show $d_{2n}^{(1)} = d_{-2n-1}^{(1)}$.

4. SIMULATIONS AND RESULTS

Image coding experiments are performed by comparing the designed length-8 and length-12 filters with the Daubechies' D8 and D12 wavelets. For fair comparisons, the same still image codec [4] was used. From the PSNR performances in Table 1, it can be concluded that the designed length-8 and length-12 filters can generally outperform the D8 and D12 wavelets by up to 0.76 dB and 0.62 dB, respectively.

Figure 3 portrays the subjective quality of the decoded 'Boat' images at a compression 32:1 using D8 and S8(1). A careful comparison reveals some distinct differences between the two images: boundary artifacts are completely removed by using symmetric extension with S8(1); and the white mast at the top center of the image and some cables are also better preserved in the reconstructed image using S8(1).

CR	D8	D12	S8(1)	S8(2)	S12(1)	S12(2)
8:1	40.57	40.64	40.74	40.75	40.73	40.77
16:1	37.14	37.25	37.40	37.43	37.38	37.46
32:1	33.88	33.96	34.25	34.29	34.22	34.30
64:1	30.84	30.84	31.33	31.39	31.30	31.39
128:1	28.18	28.14	28.73	28.75	28.72	28.76
8:1	36.73	37.19	36.86	37.05	36.83	37.04
16:1	31.53	31.91	31.62	31.79	31.59	31.78
32:1	27.70	28.01	27.88	27.98	27.87	27.97
64:1	25.02	25.11	25.23	25.26	25.22	25.26
128:1	23.53	23.58	23.71	23.72	23.71	23.72
8:1	38.48	38.47	38.73	38.76	38.73	38.77
16:1	33.84	33.84	34.12	34.16	34.11	34.17
32:1	30.28	30.33	30.60	30.61	30.59	30.62
64:1	27.60	27.59	27.89	27.87	27.89	27.89
128:1	25.48	25.51	25.76	25.76	25.76	25.77
8:1	36.10	36.10	36.31	36.34	36.31	36.35
16:1	32.61	32.60	32.88	32.90	32.87	32.90
32:1	29.97	30.03	30.39	30.40	30.38	30.40
64:1	27.88	27.95	28.38	28.39	28.37	28.40
128:1	25.91	26.08	26.65	26.67	26.64	26.65

Table 1: Image compression performance comparisons of six orthogonal filters using four 512×512 monochrome images, Lena, Barbara, Boat and Goldhill (from top to bottom).

5. CONCLUSIONS

In this paper, we investigated a special class of orthonormal wavelets. We provided the necessary and sufficient conditions to define this class, and proposed new decomposition and reconstruction algorithms for this class. We showed how this class can have smoother wavelets and yet demand lower computational cost. Then, we proved that symmetric boundary extension is applicable though the filters are non-symmetrical. Finally, we confirmed that the combined application of these special wavelets with the proposed multiresolution algorithms can result in better image compression performances.

6. REFERENCES

- [1] Daubechies I., *Ten Lectures on Wavelets*, CBMS-NSF, 1992.
- [2] Evangelista G., "Wavelet transforms and wave digital filters," *Proc. of the Int. Conf.*, Marseille, France, May, 1989.



Figure 3: Reconstructed Boat images at CR = 32:1 using (top) D8 and (bottom) S8(1).

- [3] Mallat S., "A theory for multiresolution signal decomposition: The wavelet representation," *IEEE Trans. PAMI*, 11:674-693, July, 1989.
- [4] Said A. and Pearlman W. A., "A New Fast and Efficient Image Codec Based on Set Partitioning in Hierarchical Trees," *IEEE Trans. on Circs. and Syst. for Video Tech.*, 6(3):243-250, 1996.
- [5] Strang G. and Nguyen T. Q., *Wavelet and Filter Banks*. Wellesley, MA: Wellesley-Cambridge Press, 1995.
- [6] Vaidyanathan P. P., "Multirate digital filters, filter banks, polyphase networks, and applications: A tutorial." *Proc. IEEE*, 78(1):56-93, Jan. 1990.
- [7] Vaidyanathan P. P. and Hoang P. Q., "Lattice structures for optimal design of two-channel perfect-reconstruction QMF banks," *IEEE Trans. ASSP*, vol. 36, 1988.